Early corticosteroid treatment enhances recovery from SARS-CoV-2 induced loss of smell in hamster

Laetitia Merle-Nguyen, Ophélie Ando-Grard, Clara Bourgon, Audrey St Albin, Juliette Jacquelin, Bernard Klonjkowski, Sophie Le Poder, Nicolas Meunier

Brain, Behavior, and Immunity 118 (2024) 78–89

Contents lists available at ScienceDirect

Brain Behavior and Immunity

journal homepage: www.elsevier.com/locate/ybrbi

Early corticosteroid treatment enhances recovery from SARS-CoV-2 induced loss of smell in hamster

Laetitia Merle-Nguyen [a], Ophélie Ando-Grard [a], Clara Bourgon [a], Audrey St Albin [a], Juliette Jacquelin [a], Bernard Klonjkowski [b], Sophie Le Poder [b], Nicolas Meunier [a,*]

[a] Unité de Virologie et Immunologie Moléculaires (UR892), INRAE, Université Paris-Saclay, Jouy-en-Josas, France
[b] UMR 1161 Virologie, INRAE-ENVA-ANSES, École Nationale Vétérinaire d'Alfort, Maisons-Alfort, 94704 Paris, France

ARTICLE INFO

Keywords:
Olfaction
Nasal cavity
Dexamethasone
Respiratory virus
Olfactory
Smell
Anosmia

ABSTRACT

Among the numerous long COVID symptoms, olfactory dysfunction persists in ~10 % of patients suffering from SARS-CoV-2 induced anosmia. Among the few potential therapies, corticoid treatment has been used for its anti-inflammatory effect with mixed success in patients. In this study, we explored its impact using hamster as an animal model. SARS-CoV-2 infected hamsters lose their smell abilities and this loss is correlated with damage of the olfactory epithelium and persistent presence of innate immunity cells. We started a dexamethasone treatment 2 days post infection, when olfaction was already impacted, until 11 days post infection when it started to recover. We observed an improvement of olfactory capacities in the animals treated with corticoid compared to those treated with vehicle. This recovery was not related to differences in the remaining damage to the olfactory epithelium, which was similar in both groups. This improvement was however correlated with a reduced inflammation in the olfactory epithelium with a local increase of the mature olfactory neuron population. Surprisingly, at 11 days post infection, we observed an increased and disorganized presence of immature olfactory neurons, especially in persistent inflammatory zones of the epithelium. This unusual population of immature olfactory neurons coincided with a strong increase of olfactory epithelium proliferation in both groups. Our results indicate that persistent inflammation of the olfactory epithelium following SARS-CoV-2 infection may alter the extent and speed of regeneration of the olfactory neuron population, and that corticoid treatment is effective to limit inflammation and improve olfaction recovery following SARS-CoV-2 infection.

1. Introduction

The COVID-19 pandemic is characterized by an unprecedented number of olfactory disorders cases. The first variants are responsible for up to 50 % of these symptoms (von Bartheld et al., 2021) and, while it is less frequent with the Omicron variant, ~10 % of infected patients still report olfactory disorder (von Bartheld and Wang, 2023). The disturbance of odorant perception can have a profound impact on quality of life, as this sense is essential not only for feeding behavior but also for detection of imminent danger such as gas or smoke (Meunier et al., 2021) and loss of smell is linked to an increased risk of depression and death (Van Regemorter et al., 2020). Most patients recover their olfactory capacities in a few months, but at least ~5 % still suffer from persistent olfactory disorders, including anosmia, *i.e.* a total loss of smell (Tan et al., 2022).

Loss of smell was already widespread in ~5 % of the population prior to the pandemic (Whitcroft et al., 2023), mainly related to chronic rhinosinusitis, but for about 25 % of cases to viral infection (Okumura et al., 2022). While many therapeutic options to recover from post-viral infection disorders (PVOD) have been explored since the surge in COVID-19 cases, two main treatments have emerged: olfactory training and corticoid treatment (Huart et al., 2021; Nag et al., 2023; Rashid et al., 2021; Tragoonrungsea et al., 2023; Vaira et al., 2021). Olfactory training helps to recover (Pieniak et al., 2022), but the effectiveness of corticoid treatment appears variable according to the protocol used (Hintschich et al., 2022; Hosseinpoor et al., 2022). In addition to variations in the timing of treatment after the onset of the olfactory disorder, corticoids can be used locally or systematically, which could explain their inconsistency (Pendolino et al., 2022). Most studies showing positive results conclude that larger cohorts are required to demonstrate

Abbreviations: OSN, Olfactory sensory neuron; OE, Olfactory epithelium.

* Corresponding author.
E-mail address: nicolas.meunier@inrae.fr (N. Meunier).

https://doi.org/10.1016/j.bbi.2024.02.020
Received 7 August 2023; Received in revised form 3 February 2024; Accepted 14 February 2024
Available online 15 February 2024

effectiveness (Le Bon et al., 2021).

Olfaction starts in the olfactory epithelium (OE), which contains olfactory sensory neurons (OSNs) surrounded by supporting cells called sustentacular cells. The epithelium continuously renews itself as both cell types undergoes regular apoptosis and are regenerated through multipotent basal cells (Schwob et al., 2017). We and others observed in the golden Syrian hamster model that SARS-CoV-2 massively infects the sustentacular cells in the OE, leading to its desquamation (Bryche et al., 2020; Kishimoto-Urata et al., 2022). This desquamation occurs coincident with olfactory neuron deciliation and release of these cells into the lumen of the nasal cavity, where they undergo apoptosis (Bourgon et al., 2022). It has been confirmed in humans that anosmia arises primarily from infection of the sustentacular cells of the OE followed by disruption of OE integrity without OSN infection (Khan et al., 2021). We have previously observed that innate immune cells play a major role in the destruction of the infected OE (Bourgon et al., 2022) and it has been shown that the number of resident macrophage increases as long as 42 days post infection (dpi) (Kishimoto-Urata et al., 2022). As SARS-CoV-2 infection resolves in the nasal cavity after 4 dpi (Bryche et al., 2020), the increased presence of innate immune cells in the OE persists long after the resolution of infection and may explain the delay in resolution of the olfactory disorder. These data from animal studies have been confirmed in human, since a comparative study showed a lower level of olfactory neurons and an increased presence of immune cells in OE biopsies from patients who did not recover from COVID-19-associated olfactory disorders (Finlay et al., 2022). Overall, these results indicate that persistent inflammation may be an important factor that contributes to long-lasting olfactory disorders, and that corticoid treatment should be beneficial.

As in-depth study of their effectiveness to improve COVID-19 associated olfactory disorders is difficult to achieve in humans, we used Syrian golden hamsters which display the pathophysiology of mild COVID-19, including loss of smell (Reyna et al., 2022). We treated hamsters by subcutaneous injection of dexamethasone with an anti-inflammatory dose (1.5 mg/kg) starting at 2 dpi when the animals already display smell loss (Reyna et al., 2022) and examined them at 11 dpi when olfaction starts to recover in non-treated animals.

2. Material and methods

2.1. SARS-CoV-2 isolate

In vivo experiments were carried out with SARS-CoV-2 strain BetaCoV/France/IDF/200107/2020, which was isolated by Dr. Paccoud from the La Pitié-Salpétrière Hospital in France. This strain was kindly provided by the Urgent Response to Biological Threats (CIBU) hosted by Institut Pasteur (Paris, France), headed by Dr. Jean-Claude Manuguerra.

2.2. Animals

Twenty-four 8 weeks-old male hamsters were purchased from Janvier's breeding Center (Le Genest, St Isle, France). Animal experiments were carried out in the animal biosafety level 3 facility of the UMR Virologie (ENVA, Maisons-Alfort); approved by the ANSES/EnvA/UPEC Ethics Committee (CE2A16) and authorized by the French ministry of Research under the number APAFIS#25384-2020041515287655. Weight and welfare of animals were measured and evaluated daily. Six animals were not infected and used as a control. Eighteen hamsters were infected by nasal instillation (40 μL in each nostril with $5{\cdot}10^3$ $TCID_{50}$ of SARS-CoV2 strain BetaCoV/France/IDF/200107/2020) under isofluorane anesthesia as previously described (Bourgon et al., 2022). At 2 dpi, 6 animals were euthanized to document pathophysiology prior to dexamethasone treatment. The remaining twelve animals received daily dexamethasone subcutaneously (1.5 mg/kg; Rapidexon) or the vehicle (300 μL PBS with 3.75 mg/mL benzylic alcohol). This dose was successfully used to reduce inflammation during SARS-CoV-2 infection in the hamster model (Wyler et al., 2022; Yuan et al., 2022). Nasal swabs were performed daily to measure the viral load secreted by brushing the nostrils of the animal from 1 to 5 dpi. Olfactory performance was measured 2 days prior to infection, then at 2 and 11 dpi. An extra food pellet colored in red was offered daily to measure supplementary food consumption as a sign of food intake. At 11 dpi, animals were euthanized. Heads were divided sagittally into two halves, one of which was used for immunohistochemistry experiments. The nasal turbinates and olfactory bulb were extracted from the other half for qPCR analysis.

2.3. Viral titration of nasal swabs

Nasal swabs were diluted in 400 μL of DMEM medium supplemented with 1 % sodium pyruvate and antibiotics and stored at −80 °C until titration by tissue culture infectious dose 50 % (TCID50) as described previously (Thébault et al., 2022). Briefly, each nasal swab was serially diluted within DMEM containing 1 % Sodium Pyruvate and 1 % antibiotics (Penicillin/Streptomycin) by 10^{-1} to 10^{-6} for 1 to 3 dpi and ½ and 10^{-1} for 4 and 5 dpi. After 1 h30 incubation at 37 °C with Vero E6 cells, the medium was supplemented with 5 % FCS and graded 4 days later according to an all-or-nothing scoring method for the presence of a viral cytopathic effect. Infectious titers were expressed as $TCID_{50}$ per mL according to the Spearman Karber method (Ramakrishnan, 2016).

2.4. Behavior experiments

To assess the olfactory ability of hamsters, we used the buried food test (Yang and Crawley, 2009). We found Emmental cheese to be much more attractive than the sweet food conventionally used with mice and used it as food stimulus. Hamsters get used to Emmental after leaving one small piece (10 × 4 × 2 mm) in their home cage overnight. They start actively digging for it after a single 5-min habituation session in a test cage filled with 5 cm of bedding with a piece of cheese accessible directly on the surface. This test cage was then used for two different conditions named "easy task" or "hard task", which consisted in burying the cheese at 1 or 5 cm depth respectively. Animal activity was recorded for 200 s. The time taken to find the cheese as well as the duration of activity (excluding grooming) during the task was afterwards measured by analyzing the video blind to the treatment. We could perform the two tests with a 30 min interval without any food deprivation as hamsters were always eager to harvest food. They continued to explore actively the cage even after consuming part of the founded cheese and stocked any additional food in their cheek pouches.

2.5. Histology, immunohistochemistry and quantifications

The immunohistochemistry analysis of the olfactory mucosa tissue sections was performed as described previously in mice (Bryche et al., 2019). Briefly, animal hemi-heads were fixed for 3 days at room temperature in 4 % paraformaldehyde (PFA) and decalcified in Osteosoft (101728; Merck Millipore; Saint-Quentin Fallavier; France) for 3 weeks. Blocks were cryoprotected in 30 % sucrose. Cryo-sectioning (12 μm) was performed to generate coronal sections of the nasal cavity. Sections were stored at −80 °C until use.

For immunohistochemistry, non-specific staining was blocked by incubation with 2 % bovine serum albumin (BSA) and 0.1 % Triton. Sections were then incubated overnight with primary antibodies directed against SARS Nucleocapsid protein (1/1000; mouse monoclonal; clone 1C7C7; Sigma-Aldrich), ionized calcium-binding adapter molecule 1 (Iba1) (1/500; rabbit monoclonal; clone EPR16588; Abcam), Olfactory Marker Protein (OMP) (1/1000; goat polyclonal; 544–10001; Wako); GAP43 (1/500; rabbit polyclonal; NB300 143; Novus); Arg1 (1/200; rabbit polyclonal; PA5-29645; Thermofisher); Ki67 (1/100; Rabbit polyclonal; MA139550; Thermofisher) and cleaved caspase 3 (1: 400; rabbit polyclonal, Cell Signaling; Ozyme). Fluorescence staining was

performed using donkey anti-mouse-A555; donkey anti-rabbit-A488 and donkey anti-goat-A546 (1/800; Molecular Probes A-31570; A32790; A-11056 respectively; Invitrogen).

To assess the impact of corticoid treatment on the OE after SARS-CoV-2 infection, we focused our measures on coronal sections of nasal turbinates in the middle of the nasal cavity, containing the NALT and the end of Steno's gland (Supp Fig. 1). We choose this area as it presents two zones behaving differentially for the recovery of OE damage following SARS-CoV-2 infection (Kishimoto-Urata et al., 2022).

To measure olfactory epithelium damage, we performed conventional hematoxylin and eosin (HE) staining as previously described (Bourgon et al., 2022) and scored slices from 1 to 9 according to OE thickness, irregularities, missing areas and presence of cellular debris in the lumen of the nasal cavity.

We examined the presence of $Iba1^+$ cell in both lamina propria and OE, as well as $GAP43^+$ and OMP^+ cells in the OE to assess immune cell infiltration, the presence of immature olfactory neurons and mature olfactory neurons, respectively. For each animal, we quantified the presence of $Iba1^+$ and OMP^+ cells based on 4 images in the dorso median and in the ventro lateral part of the OE. We measured the percentage of stained area with ImageJ (Rasband, W.S., ImageJ, U.S. National Institutes of Health, Bethesda, Maryland, USA, http://imagej.nih.gov/ij/, 1997–2012) in the lamina propria for Iba1 staining and in the middle part of the OE layer (~50 %) for OMP staining as it holds the mature neurons layer (Moon et al., 2002). For $GAP43^+$ immature olfactory neurons, we scored a level of disorganization from 1 to 9 based on the presence of staining in the same middle part (~50 %) of the OE layer, where immature olfactory neurons are normally absent (Moon et al., 2002). For Ki67 and C3C staining, we scored the presence of cells in the OE from 0 (absence) to 9 (ubiquitous). For Arg1 and Iba1 co-staining, we measured the ratio of $Arg1^+Iba1^+$/ $Iba1^+$ cells in the olfactory mucosa (containing both lamina propria and olfactory epithelium) in the dorso median region of the OE. Glomerular size in the olfactory bulb was measured based on OMP staining with ImageJ. For each animal, two different slices approximatively separated by 500 μm were analyzed. The size of the 4 largest glomeruli on both slices were averaged per animal and normalized to the average glomerular size of control animals.

Images for all fluorescent IHC were taken using an Olympus 1X71 microscope equipped with an Orca ER Hamamatsu cooled CCD camera (Hamamatsu Photonics France; Massy; France). Whole sections of nasal cavity HE staining were reconstructed from 2 images taken at x30 magnification using a Leica MZ10F binocular microscope.

2.6. RNA extraction and RT-qPCR analysis

Total RNA was extracted from frozen nasal turbinates using the Trizol-chloroforme method as described previously (Bryche et al., 2019). Oligo-dT first strand mixed with random hexamers cDNA synthesis was performed from 1 μg total RNA with the iScript Advance cDNA Synthesis Kit for RT-qPCR (Bio-Rad; #1725038) following the manufacturer's recommendations. qPCR was carried out using 25 ng of cDNA added to a 15 μL reaction mix containing 10 μL iTaq Universal Sybr Green SuperMix (BioRad; #1725124), and primers at 500 nM (sequences in Supp Table 1). The reaction was performed with a thermocycler (Mastercycler ep Realplex, Eppendorf). Fluorescence during the qPCR reaction was monitored and measured by Realplex Eppendorf software. A dissociation curve was plotted at the end of the forty amplification cycles of the qPCR to confirm the ability of theses primers to amplify a unique and specific PCR product.

Quantification of the initial concentration of specific RNA was achieved using the *ΔΔCt* method. Standard controls for qPCR specificity and efficiency were performed. The mRNA expression of each gene was normalized with the expression level of Dicer. A correction factor was applied to each primer pair according to their efficiency (Muller et al., 2002). Data are presented as relative expression level compared to uninfected animals in the olfactory turbinates and to vehicle in the olfactory bulb.

2.7. Statistical analysis

All comparisons were made using Prism 8.0 (GraphPad). Statistical significance between groups was assessed using non-parametric Mann Whitney tests. For correlation analyses, we used Spearman's non-parametric test. Error bars indicate the SEM. Multivariate statistical analysis on RNA levels in nasal turbinates was achieved using Principal Component Analysis (PCoA) with R software. Detailed information on statistical test used, sample size and P value are provided in the figure captions.

3. Results

3.1. Pathophysiological impact of early corticoid treatment on SARS-CoV-2 infection

In order to examine how an early treatment with corticoids could improve the recovery of loss of smell induced by SARS-CoV-2 infection, we treated hamsters from 2 dpi to 11 dpi with daily subcutaneous injection of 1.5 mg/kg of dexamethasone (Fig. 1A). We started the treatment at 2 dpi because most of the damage of the OE has already been initiated in the nasal cavity (Bourgon et al., 2022) and a very strong loss of olfactory abilities is observed in hamsters at this early stage (Reyna et al., 2022). We stopped the treatment at 11 dpi when about 50 % of the OE should have regenerated (Bryche et al., 2020), making it a suitable time window to observe early improvements in OE repair due to corticoid treatment. $TCID_{50}$ from nasal swabs taken between 1 and 5 dpi were not statistically different in the dexamethasone and vehicle-treated groups, indicating that the treatment starting at 2 dpi did not impact the level of infection in the nasal cavity (Fig. 1B). Hamster weight decreased following infection with a maximum loss of ~7 % at 6 dpi and a recovery at 11 dpi regardless of dexamethasone treatment (Fig. 1C). We measured food intake also indirectly by introducing an extra-colored food pellet left on the bedding surface of the animal home cage overnight. The decrease of extra food consumption was similar to the weight loss during the course of infection with a maximal decrease at 5 dpi (Fig. 1D). However, animals treated with dexamethasone statistically consumed more extra food than those treated with the vehicle as early as 2 days post corticoid treatment (Two-way ANOVA; $F_{(1,\ 110)} = 5.458$; $P = 0.0213$) but this was similar at 11 dpi when we measured their olfactory capacities. We also measured their olfactory abilities using a slightly modified buried food test involving two different depths of hidden food (Fig. 2). At 2 dpi, we observed a significant decrease of olfactory performances with shallow or deeply buried food, consistent with a previous study (Reyna et al., 2022). Both the vehicle and Dexamethasone-treated animals showed a partial recovery of their ability to discover shallow buried food at 11 dpi. Indeed, at 11 dpi animals from both groups spent significantly more time to retrieve the hidden food than prior to infection (Mann Whitney, $P = 0.0022$ and 0.0173 for vehicle and dexamethasone groups, respectively). When the food was deeply buried, both groups were significantly less efficient at 11 dpi than prior to infection and did not perform better than at 2 dpi. However, the dexamethasone-treated group performed significantly better than the vehicle group with 5 vs 1 out of 6 animals finding the food respectively (Fig. 2C; Mann Whitney, $P = 0.0291$), indicating that the olfactory function was improved by the corticoid treatment. The percentage of activity during the food buried test was similar for both groups (Fig. 2C).

3.2. Change in genes expression related to odor detection and immune response

The expression of olfactory transduction-related genes in the OE has been shown to be markedly decreased following SARS-CoV-2 infection

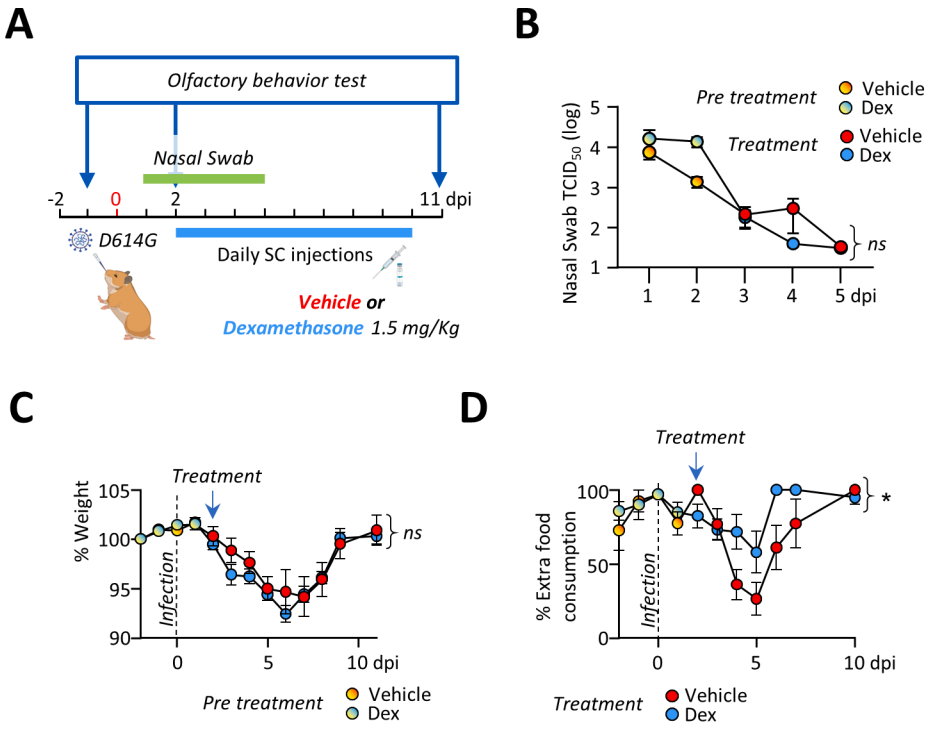

Fig. 1. Pathophysiological impact of early corticoid treatment on SARS-CoV-2 infection. *(A) Experimental design to evaluate the treatment of SARS-CoV-2 infected hamsters with sub-cutaneous (SC) corticoid treatment started at 2 dpi until 11 dpi (days post infection) (B) Viral load in nasal swab collected from 1 to 5 dpi (C) Weight monitoring (D) Extra food consumption as an indirect measure of food intake (Mean ± SEM, n = 6, 2-way ANOVA followed by Bonferroni post-test; ns: P > 0.05; * P < 0.05).*

in mice (Verma et al., 2022). Most volatile odorants are transduced through the activation of an olfactory receptor (OR) coupled to a specific G protein G_{olf}, which in turn activates the adenylate cyclase III. The increase in cAMP level in turn activates a CNG channel (Cnga2), and the concentration of cAMP is buffered by the olfactory marker protein present only in mature olfactory neurons (OMP; Nakashima et al., 2020). We observed that, contrary to mice, the expression level of all olfactory transduction-related genes was not significantly affected at 2 dpi compared with uninfected animals (Fig. 3A). However, their expression was strongly decreased at 11 dpi without any significant impact of the corticoid treatment. We then examined the population of immature neurons using the expression level of GAP43 (Verhaagen et al., 1989). Again, its level was unaffected at 2 dpi, but increased statistically at 11 dpi without impact of the corticoid treatment (Fig. 3A). This increase could be linked to proliferation of basal cells, and we therefore measured the expression level of Ki67 related to cellular division (Ohta and Ichimura, 2000). The alteration of its level was consistent with GAP43. Several studies in animal models and humans have shown a long-term persistence of inflammation in the olfactory system and different brain parts following SARS-CoV-2 infection. This has been shown notably by an increased presence of $Iba1^+$ cells; a marker of microglia in the brain including the olfactory bulb and activated macrophages in the olfactory turbinates (Finlay et al., 2022; Kishimoto-Urata et al., 2022; Rutkai et al., 2022). Furthermore, we previously observed an increase in the innate immune cell population as early as 1 dpi (Bourgon et al., 2022). We thus measured the expression level of $Iba1^+$ (related to resident macrophages), Ncf2 (related to neutrophils) and CD68 (related to circulating macrophages). While all these genes were overexpressed at 2 dpi, their levels were significantly reduced at 11 dpi, with only CD68 related to circulating macrophages being statistically decreased by the corticoid treatment (Fig. 3A). We also measured the expression level of CD163 and CD206, markers of anti-inflammatory M2 macrophages (Etzerodt and Moestrup, 2013; Jablonski et al., 2015). Both levels were increased following SARS-CoV-2 infection but their level was higher in the corticoid treated group at 11 dpi (Fig. 3A). Consistent with the anti-inflammatory property of corticoid treatment, we also observed a significant decrease of IL6 expression levels in the olfactory turbinates and olfactory bulb of the dexamethasone group (Fig. 3B, C). While many markers were not statistically affected by the corticoid treatment, such as CXCL10 and IL10, we observed a tendency of decreased inflammation markers and improved olfactory marker following the treatment. We thus performed a principal component analysis showing that animals treated with corticoid clearly form a distinct group from those treated with vehicle alone (Fig. 3D).

3.3. Corticoid treatment reduces resident macrophages presence in the olfactory mucosa following SARS-CoV-2 infection

Prolonged inflammation following SARS-CoV-2 infection has been well characterized in the nasal cavity (Bryche et al., 2020; Finlay et al., 2022; Kishimoto-Urata et al., 2022). Among the different immune cells present during early inflammation of the infected olfactory epithelium, we previously observed a massive presence of $Iba1^+$ resident macrophages as well as $CD68^+$ circulating macrophages and MPO^+ neutrophils. $CD68^+$ and MPO^+ cells were mainly observed during the phases of the epithelial damage (Bourgon et al., 2022). Among these innate immune cells, we observed only the persistence of $Iba1^+$ cells at 11 dpi and thus focus our attention on them. The persistent presence of these cells in the olfactory turbinates after SARS-CoV-2 infection has been shown to be spatially restricted (Kishimoto-Urata et al., 2022). While their presence in the ventro lateral part of the OE returns to its basal state at 21 dpi, the dorso median zone has been shown to stay inflammatory and damaged up to 42 dpi (Kishimoto-Urata et al., 2022). To assess the effectiveness of the corticoid treatment following SARS-CoV-2 infection on the recovery of the OE in the nasal cavity, we focused on a coronal section in the middle of the nasal cavity where we found similarly a sustained presence of $Iba1^+$ cells in both the dorso median part and the ventro lateral zone of the nasal cavity (Fig. 4). At 11 dpi, $Iba1^+$ cells were mainly present in the lamina propria and at a higher level than prior to infection for both areas in vehicle-treated animals (Fig. 4C;

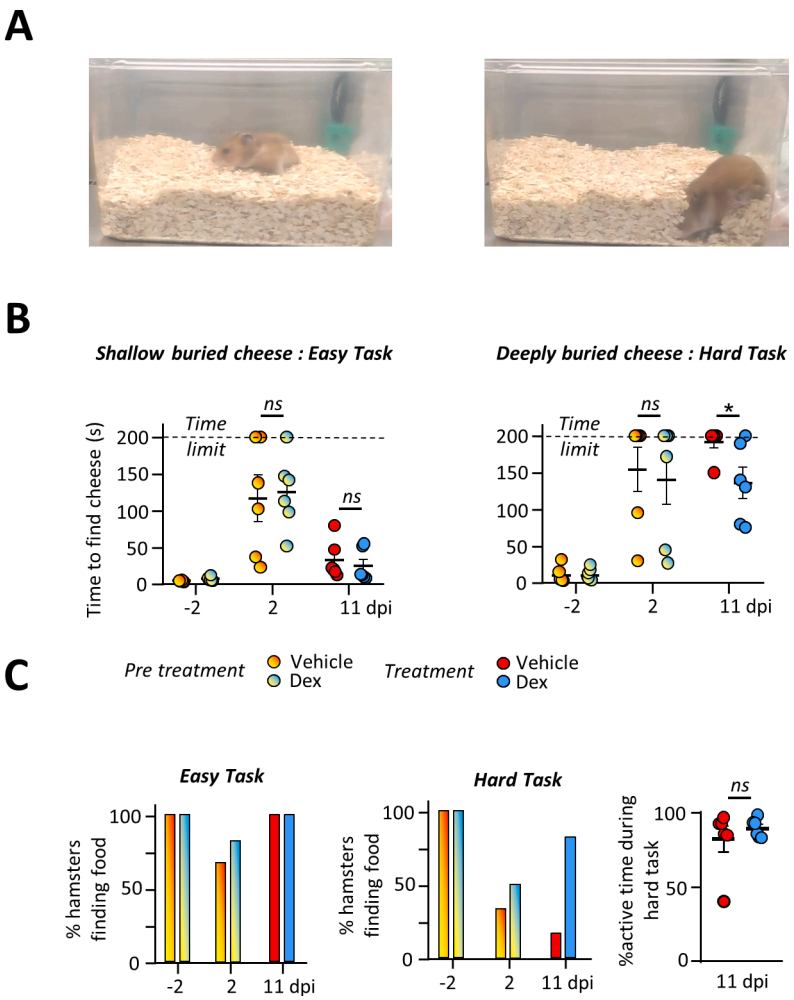

Fig. 2. Monitoring of olfactory abilities of SARS-CoV-2 infected hamsters treated early with corticoids (A) *Representative images of a hamster scanning the surface for food (left) and digging for a deeply buried piece of cheese (right) (B) Amount of time taken and (C) percentage of hamsters finding a shallow or deeply buried piece of cheese (left and middle panel respectively) and percentage of active time during the hard task (right panel). 2 days before infection, at 2 dpi just before corticoid treatment and at 11 dpi after daily corticoid (Dex) or vehicle treatment (Mean ± SEM, n = 6, Mann Whitney; ns: P > 0.05; * P < 0.05). The animal has 200 s to find the food before the test ends.*

Mann-Whitney, P < 0.0001 for both zones). The dexamethasone treatment significantly decreased their presence in both zones compared to vehicle-treated animals. However, the level remained higher than before infection in the dorso median part (Fig. 4C; Mann-Whitney, P < 0.0001). As the M2 macrophages markers CD206 and CD163 were significantly more expressed in the corticoid treated group, we investigated the presence of Arg1 in the olfactory turbinates which is another M2 macrophage marker (Yang and Ming, 2014). Most of the $Arg1^+$ cells were also $Iba1^+$ at 11 dpi and we observed an increased ratio of $Arg1^+$/$Iba1^+$ cells in the corticoid treated group (Supp. Fig. 1).

3.4. Corticoid treatment impact on the olfactory neuron population after SARS-CoV-2 infection

Following SARS-CoV-2 infection of sustentacular cells in hamsters, massive damage occurs in the epithelium, resulting in the loss of olfactory neurons into the lumen of the nasal cavity (Bourgon et al., 2022; Bryche et al., 2020). We chose 11 dpi as we expect that approximatively 50 % of the epithelium would have regenerated, based on previous study of the regeneration time course (Bryche et al., 2020; Reyna et al., 2022) and that corticoid treatment could improve such recovery. Indeed, prolonged inflammation has been shown to hamper the regeneration of the olfactory epithelium (Chen et al., 2019) and we observed that the treatment effectively limited inflammation in the olfactory mucosa (Figs. 3 and 4). We first examined the recovery from damage in the olfactory epithelium based on histological staining. We did not observe statistical difference between vehicle and corticoid-treated animals (Supp. Fig. 2). We next examined the regeneration level of the olfactory epithelium based on Ki67 staining (Ohta and Ichimura, 2000). While the level was much higher than in the control uninfected animal, it was again not affected by the corticoid treatment (Fig. Supp 3).

We next focused on the olfactory neuron population, and first on immature neurons specifically expressing GAP43 (Verhaagen et al., 1989). In control animals, the cell bodies of immature neurons were mainly present in the basal part of the epithelium and formed only a few layers (Fig. 5). At 11 dpi, we observed unusual multi layers of staining with cell bodies also present in the apical part of the epithelium in vehicle and corticoid-treated animals. We thus scored the degree of disorganization of GAP 43 staining to evaluate if the corticoid treatment could improve the organization level of immature neurons. While we observed that the disorganization was higher in the dorso median part of the olfactory turbinates, we did not observe any statistically significant effect of the corticoid treatment.

We then measured if the corticoid treatment could have locally impacted the mature olfactory neuron population based on OMP immunostaining specifically expressed in these cells (Nakashima et al., 2020). We observed in vehicle-treated animals, that at 11 dpi the mature olfactory neuron population was strongly reduced compared to control,

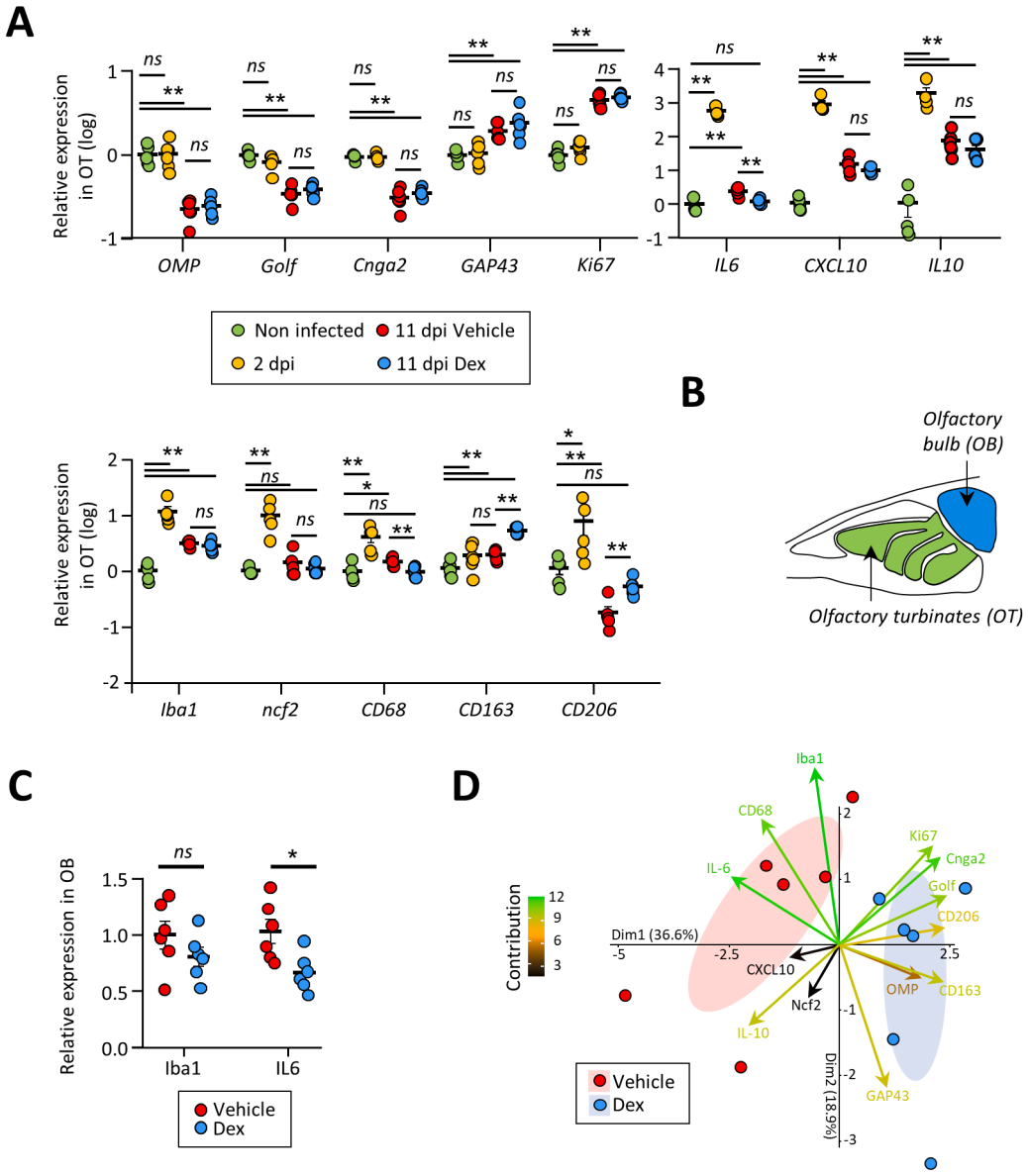

Fig. 3. Molecular impact on the olfactory system of SARS-CoV-2 infected hamsters treated by early corticoids *(A) Expression level of genes related to olfactory transduction and inflammation in the olfactory turbinates of animals; uninfected (CTL); at 2 dpi corresponding to the start of the corticoid treatment and at 11 dpi after treatment with vehicle or dexamethasone (Dex) (B) Schematic of an hamster hemi head anterior part showing the localization of the olfactory turbinates and olfactory bulb. (C) Expression level of genes related to inflammation in the olfactory bulb of animals at 11 dpi after treatment with vehicle or dexamethasone (Dex). Relative expression means ± SEM, n = 6, Mann Whitney; ns: P > 0.05; *P < 0.05; **P < 0.01. (D) PCoA biplots of RNA levels in olfactory turbinates. Each dot represents a separate animal, colored according to the treatment. Ellipses represent a confidence interval of 95 %. Arrows color and their direction toward the ellipses center reflect the contribution of the corresponding gene to the first two components of PCoA. The two groups differ significantly (permutational multivariate analysis of variance with adonis, P < 0.005).*

especially in the dorso median part of the olfactory turbinates where OMP signal was mostly absent (Fig. 6A). While we observed a slightly better OMP signal in the dorso median part for some dexamethasone-treated animals, the group was not statistically different from vehicle-treated animals. We however observed a significant increase in OMP stained cells in the ventro lateral part of the olfactory turbinates compared to vehicle-treated animals (Fig. 6C).

To confirm this result, we took advantage of the OMP expression in the axons of olfactory neurons. As these axons converge in the olfactory bulb, the OMP staining can be seen in the glomeruli which collect axons from neurons expressing the same olfactory receptor. The size of the glomeruli reflects the olfactory neuron population in the olfactory epithelium (Bozza et al., 2002). We thus measured the size of glomeruli based on OMP staining as a global measure of the olfactory neuron population. While the size was decreased for both groups compared to uninfected animals, it was higher in dexamethasone-treated animals (Fig. 7A, B). We also found a significant correlation between the glomerular size of animals and their time to find the buried food (Fig. 7C).

We finally examined if this difference in olfactory mature neuron population could be related to a higher level of apoptosis in the olfactory epithelium by measuring the level of cleaved caspase 3 staining (Porter and Janicke, 1999). We did not observe any statistical difference between uninfected animals and vehicle or corticoid-treated animals for both zones of the olfactory epithelium (Supp. Fig. 3).

4. Discussion

As the number of patients suffering from long term olfactory disorder increases, animal models are necessary to assess the effectiveness of

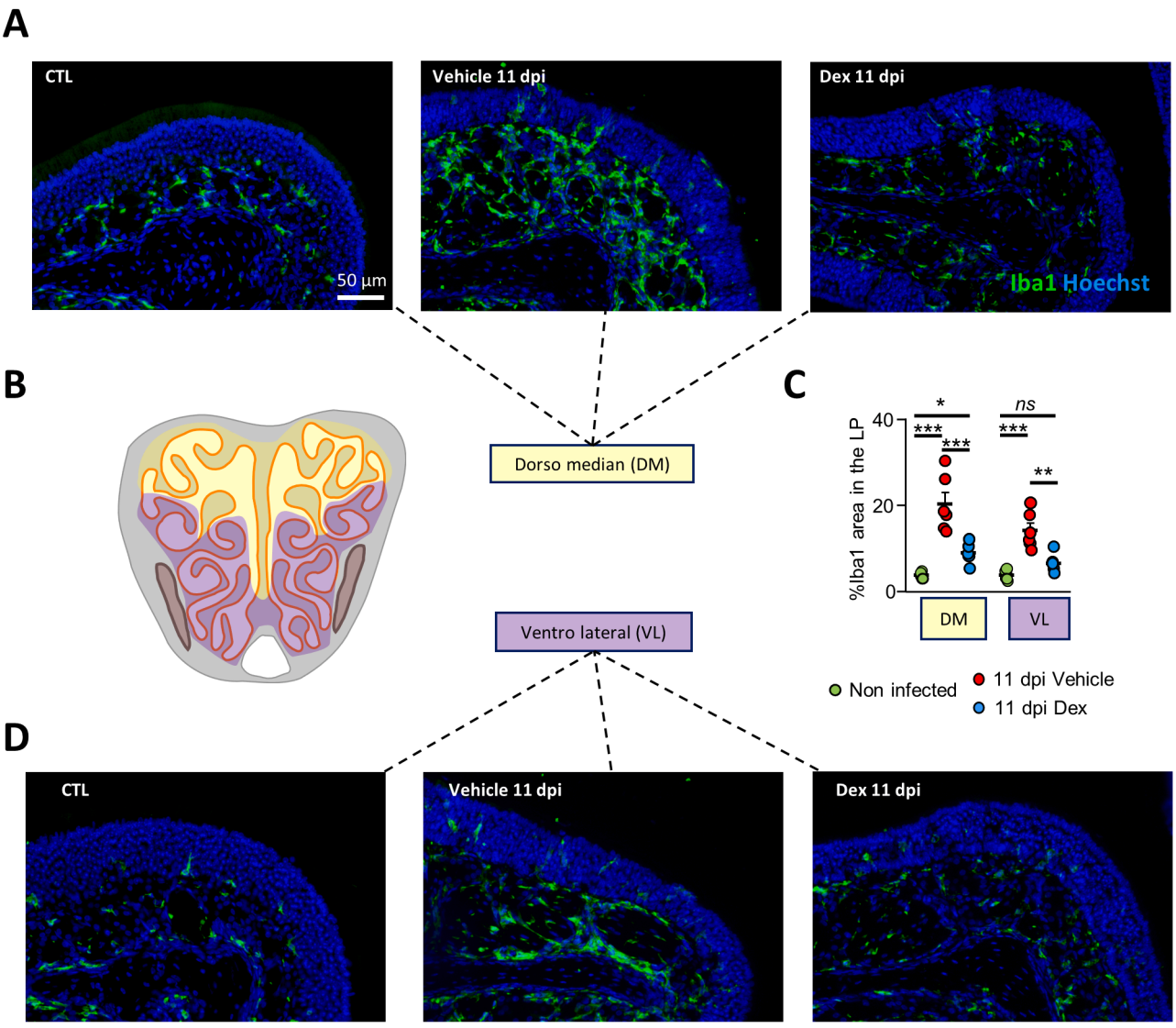

Fig. 4. Reduction of resident macrophage presence in the olfactory mucosa of SARS-CoV-2 infected hamsters treated with corticoids. *Representative images of olfactory turbinates in the dorso median (A) or ventro lateral (D) part of a coronal section in the middle of the nasal cavity (B). (C) Iba1 staining related to resident macrophage presence in the lamina propria (LP). Mean ± SEM, n = 6, Mann Whitney; *P < 0.05; **P < 0.01; ***P < 0.0001; ns non-significant.*

therapeutic treatments such as corticoid which have variable effectiveness in humans. Using Syrian golden hamsters, our results show that early systemic corticoid treatment is effective in improving olfactory recovery following SARS-CoV-2 infection.

We started the corticoid treatment at 2 dpi, when the infection is still going on. As corticoids have an anti-inflammatory effect, it may increase the level of viral infection. Such treatment started at 2 dpi has already been tested in SARS-CoV-2 infected hamsters using similar dose of dexamethasone (Wyler et al., 2022). While the authors focused on lung physiopathology, they observed a beneficial anti-inflammatory effect and a non-significant slight increase of viral burden in the lungs. Our results of viral titration from nasal swabs indicate similarly that the dexamethasone treatment when started at 2 dpi did not impact the viral presence in the nasal cavity (Fig. 1B). The similar weight loss observed in both groups indicates as well that it did not change strongly the pathophysiology of the infection (Fig. 1C). In order to characterize the olfactory performances of hamsters, we used a buried food test. This test is classically performed with only one level of buried food (Yang and Crawley, 2009) but we chose to do it with the food buried at two different levels. Interestingly, at 2 dpi, 75 % of hamsters were still able to find a shallow buried piece of cheese (Fig. 2B), indicating that most were hyposmic. This result contrasts with a previous study where hamsters have been reported to be anosmic at 2 dpi (Reyna et al., 2022) but consistent when using only the deeply buried food. Indeed, in this condition, we observed that only 33 % of hamsters could find the food, which could indicate that most are anosmic (Fig. 2C). It may thus be relevant to perform the food buried test at these two levels to better characterize the olfactory disorder in rodent models. Interestingly, we observed that food intake, which strongly decreases at 4 dpi in the vehicle group was much less impacted in the group treated with corticoid (Fig. 1D). This increase of food intake is consistent with the improved olfactory capacities observed at 11 dpi in this group, as olfaction is essential for food intake in rodents. It may also be related to the direct impact of corticoid on food intake (Dallman et al., 2004), but the consumption of extra food was similar in both groups at 11 dpi when olfaction is also recovered for an easy task in the vehicle-treated group. Such a result raises the question of the importance of olfaction in the weight loss following SARS-CoV-2 infection in hamsters.

A recent study in mice shows that following infection with a mouse adapted SARS-CoV-2, there is an important impact on gene expression related to olfactory transduction (Verma et al., 2022). Similar results have been observed in hamsters using single-cell RNA seq as early as 1

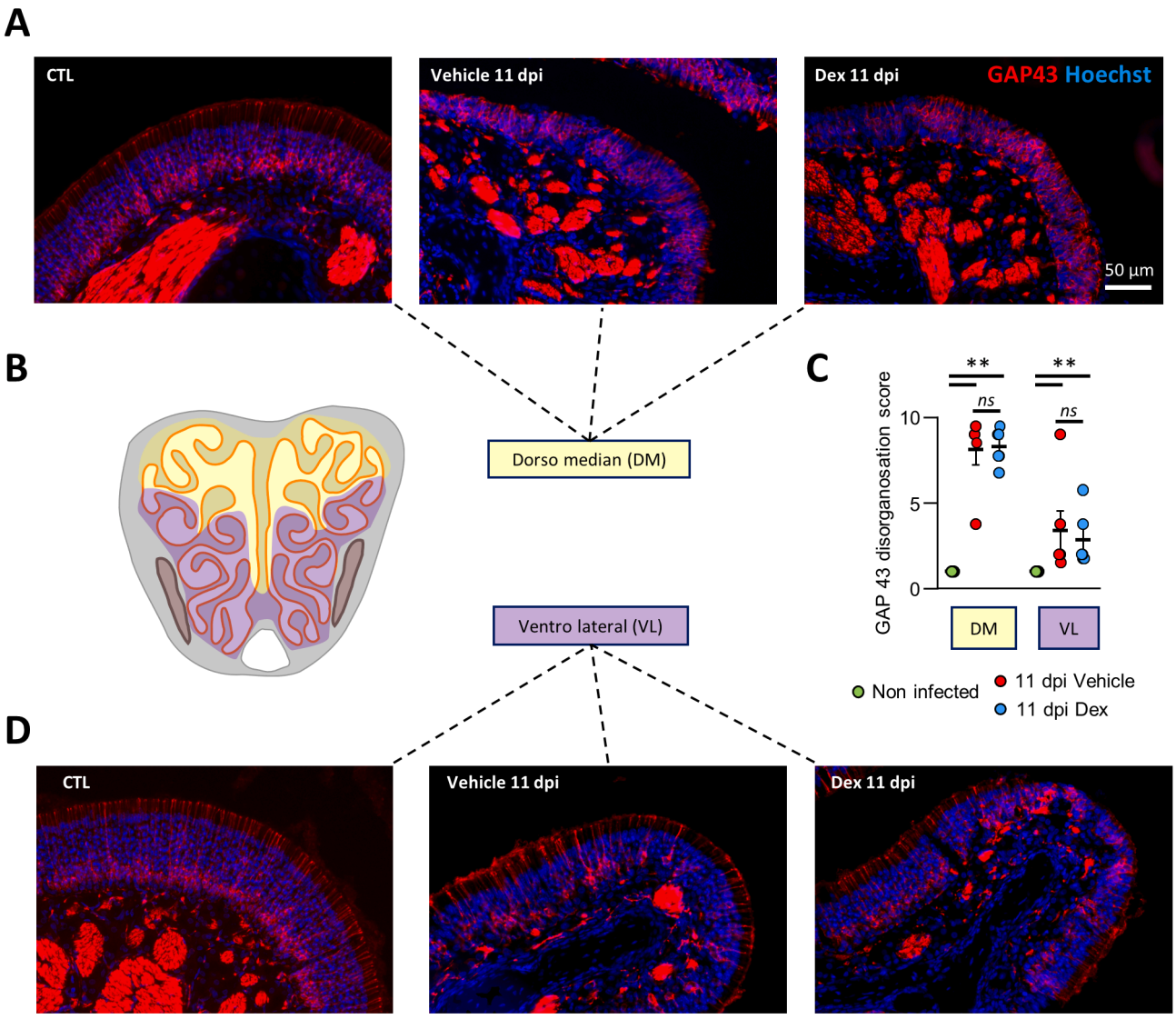

Fig. 5. Disorganization of immature olfactory neuron population at 11 dpi in vehicle and corticoid treated animals. *Representative images of olfactory turbinates in the dorso median (A) or ventro lateral (D) part of a coronal section in the middle of the nasal cavity (B). (C) Scores of the degree of disorganization of immature olfactory neuron population based on GAP43 staining. Mean ± SEM, n = 6, Mann Whitney; *P < 0.05; **P < 0.01; ns non-significant.*

dpi (Zazhytska et al., 2022). Surprisingly, while we observed a decrease in hamster olfactory capacities at 2 dpi, we did not find any impact on the expression of genes related to olfactory transduction (Fig. 3A). Such result is consistent with histological data showing that at 2 dpi, most of the OE in the posterior nasal cavity is still spared from damage (Bourgon et al., 2022). We can thus hypothesize that the loss of smell at 2 dpi may be rather related to either cellular debris in the lumen of the nasal cavity, which could impair air flow and thus odorant detection, massive loss of olfactory sensory neuron cilia (Bryche et al., 2020), or disruption of the sustentacular cells, which are essential for odorant detection (Butowt et al., 2023), but not yet to olfactory neuron loss. At 11 dpi, the expression of all genes related to olfactory transduction was strongly diminished, which could explain the persistence of hyposmia in both groups. The expression of genes related to inflammation and innate immunity cells presence in the OE was also strongly increased at 2 dpi. This expression globally decreased at 11 dpi but remained at a higher level than control for all genes, except ncf2, which is related to neutrophil presence. This higher level of gene expression related to inflammation and immune cell infiltration at 11 dpi is consistent with the persistence of inflammation reported previously in humans and hamsters (Finlay et al., 2022; Kishimoto-Urata et al., 2022). The corticoid treatment was effective to reduce the expression of CD68, related to macrophages presence, as well as the inflammatory cytokine IL6 in the OE and olfactory bulb (Fig. 3C). The lower presence of markers related to immune cells presence in the OE was confirmed by histology, showing a decreased presence of Iba1$^+$ cells in the olfactory mucosa (Fig. 4). We also measured an increase in CD163 and CD206 expression; markers of M2 anti-inflammatory macrophages (Etzerodt and Moestrup, 2013; Orecchioni et al., 2019). This is consistent with the known CD163 overexpression following corticoid treatment (Takenouchi et al., 2021). Arg1 is another M2 macrophage marker (Orecchioni et al., 2019) and we observed an increased ratio of double stained Arg1/Iba1 cells (Supp. Fig. 1). Iba1$^+$ cells are poorly described in the nasal cavity. We previously observed that they do not express CD68 contrary to macrophages invading the olfactory turbinates following SARS-CoV-2 infection (Bourgon et al., 2022) and thus characterized the Iba1$^+$ cells as resident macrophages. The elevated ratio of Arg1 co-expression following dexamethasone treatment show that the Iba1$^+$ cells can also evolve toward an M2 macrophage phenotype. While, these cells need to be further characterized, our observations are consistent with the anti-inflammatory action of corticoid and may explain the improved olfactory abilities in the dexamethasone-treated group for the buried food

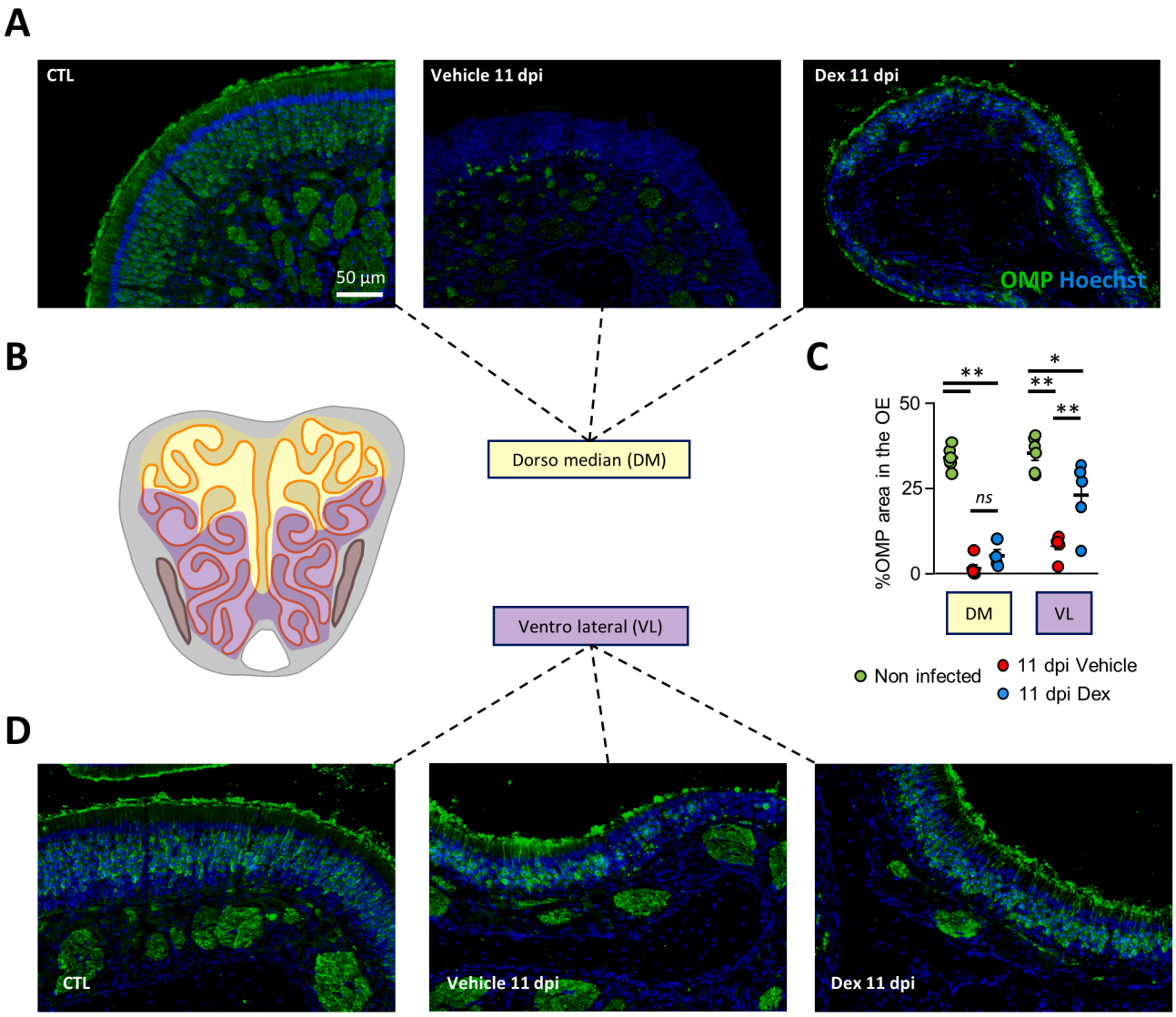

Fig. 6. Local improvement of the mature olfactory neuron population at 11 dpi in SARS-CoV-2 infected hamsters treated with corticoids. *Representative images of olfactory turbinates in the dorso median (A) or ventro lateral (D) part of a coronal section in the middle of the nasal cavity (B). (C) OMP staining related to the mature olfactory neuron population. Mean ± SEM, n = 6, Mann Whitney; *P < 0.01; **P < 0.001; ns non-significant.*

test. It could be interesting to investigate if this effect relies mainly on IL6 reduction level but it would require another animal model as available tools in hamsters to block IL6 are unfortunately limited.

Prolonged inflammation has been shown to hamper the renewal of the olfactory epithelium (Chen et al., 2019), which could thus limit the regeneration of the OE following the massive desquamation caused by SARS-CoV-2 infection (Bryche et al., 2020). Despite the persistence of inflammation, we observed a strong increase in cellular proliferation consistent with an increased level of GAP43 expressed by immature olfactory neurons (Fig. 3A; 5 and Supp. Fig. 2). The presence of immature olfactory neurons was confirmed by histology, with a strong zonal difference. Their population had almost returned to the uninfected level in the ventro lateral zone of the nasal cavity but was strongly altered in the dorso median part. In control animals, the cell bodies of immature olfactory neurons are restricted to the basal part of the OE (Moon et al., 2002), and they project a typical dendrite extension toward the apical part of the OE with a dendritic knob. Such organization was lacking at 11 dpi in the dorso median part of the nasal cavity (Fig. 5). Interestingly, similar results have been observed 2 weeks after methimazole treatment inducing a complete desquamation of the OE (Bergman et al., 2002). The zone of the disorganization of immature olfactory neuron population correlates with the higher presence of iba1^{+} cells (Fig. 4). This differential presence of Iba1^{+} cells has already been reported, as late as 42 dpi, in hamsters OE and was associated with a loss of olfactory mature neurons (Kishimoto-Urata et al., 2022). We found a similar result with an absence of OMP staining in the OE of vehicle-treated animals at 11 dpi in the dorso-median zone, which was partially restored by the corticoid treatment (Fig. 6). The increase of the mature olfactory neuron population by the dexamethasone treatment was consistent with the size of glomeruli in the olfactory bulb. Indeed, glomerular size reflects the amount of innervating OE olfactory neurons (Bozza et al., 2002). Furthermore, the glomerular size in the olfactory bulb was correlated with the hamster's performance in the hard task of the buried food test (Fig. 6C). Interestingly, the size of olfactory bulb in patients suffering from long-lasting olfactory disorders following SARS-CoV-2 infection is reduced (Frosolini et al., 2022). Such reduction is consistent with a reduced mature olfactory neuron population in the OE observed in human biopsies of patients suffering from non-recovering COVID-19 hyposmia (Finlay et al., 2022). How could the diminishing inflammation help the recovery of the mature olfactory neuron population? Inflammation may either impair the differentiation of immature neurons to mature neurons or increase the level of neuronal death related to tissue

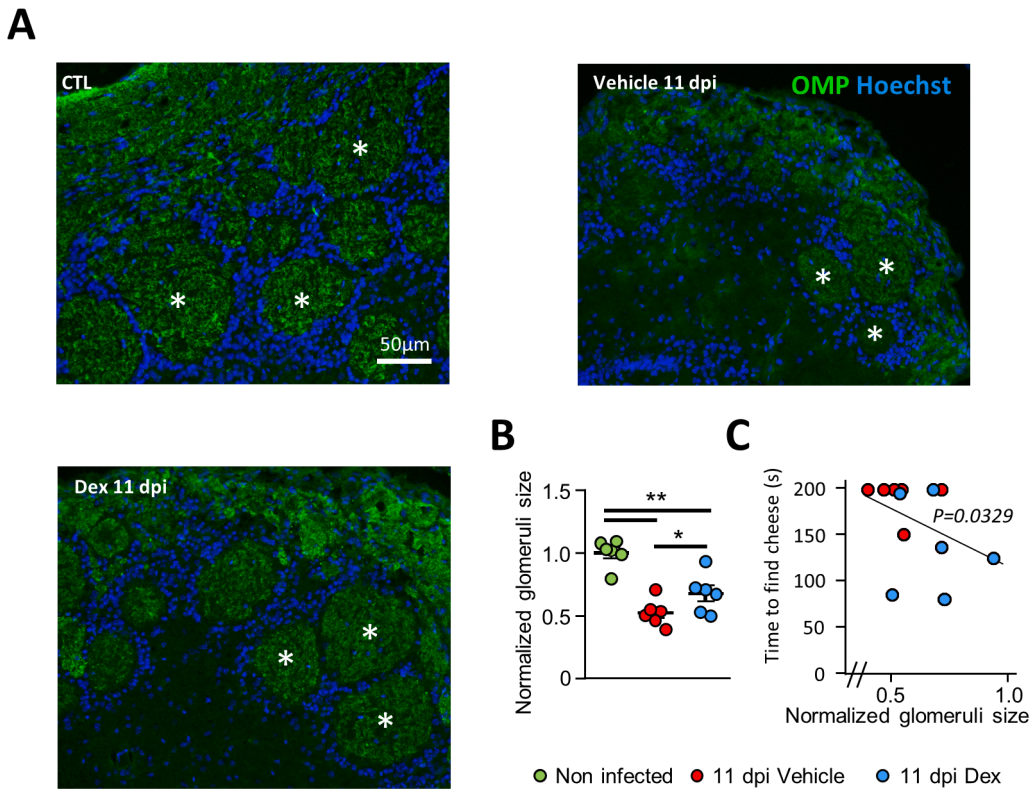

Fig. 7. Improvement of glomerular size at 11 dpi in SARS-CoV-2 infected hamsters treated with corticoids. *(A) Representative images of olfactory bulb periphery containing glomeruli (white asterisk) stained by OMP present in the converging axons of mature olfactory neurons. (B) Mean of normalized glomerular size ± SEM, n = 6, Mann Whitney; *P < 0.05; **P < 0.01. (C) Correlation between the time taken by one animal to find buried food and the average size of its glomeruli in the olfactory bulb. Spearman test* p *value.*

damage. While we did not observe different levels of apoptosis at 11 dpi in both groups (Supp. Fig. 2), it could be related to pyroptosis or necrosis even if such cellular deaths are not yet described in the OE even during high inflammation (Suzuki and Farbman, 2000). We would need to examine earlier time points to decipher how corticoid treatment helps to restore the mature olfactory neuron population. While hamster basic olfaction has already recovered at 11 dpi as can be seen by the good performance of the vehicle-treated group in the easy food buried task (Fig. 2), only the group treated with corticoid could partially recover their capacity to smell a deeply buried food. How can the animals perform a basic olfactory task when their mature olfactory neuron population is very low? Indeed, we observed in vehicle treated group that the OMP score level is at best around 10 % of prior infection level in the most preserved zone of the OE. It has been hypothesized than 10 % of original olfactory neuron population may be enough for basic olfaction discrimination so hamster olfactory neuron population might still be around this threshold at 11 dpi (Butowt et al., 2023). Another possibility is that immature olfactory neurons may be already efficient to transmit pertinent olfactory information. Indeed, it has been shown recently that 5 days old immature neurons allows mice to perform olfactory discrimination task (Huang et al., 2022) and hamsters olfactory epithelium may hold such immature neurons at 11 dpi. Furthermore, the fact that we observed a progressive recovery of olfactory performances in hamsters raises the question of the recovery evaluation of the smell capacities in humans. Indeed, UPSIT (University of Pennsylvania Smell Identification Test) is the most used olfactory test and consists at directly smelling different odors presented under the nose (Doty et al., 1984). As humans have a very good sense of smell (McGann, 2017), it may be that the olfactory disorder following SARS-CoV-2 infection lasts far longer than currently estimated, as it would require more sophisticated tests to measure the real olfactory capacities.

So far, most corticoid treatment has been performed in humans when the olfactory disorder does not recover spontaneously several weeks post-infection (Huart et al., 2021; Le Bon et al., 2021; Vaira et al., 2021; Nag et al., 2023). Only one has been performed within one week after the onset of COVID-19-related olfactory disorders. In this study, the authors did not observe any impact of the corticoid treatment which was performed by nasal irrigation (Tragoonrungsea et al., 2023). Oral administration may be more effective in humans as nasal irrigation requires specific posture to reach the olfactory cleft (Mori et al., 2016). Rodents model may not be a good model to explore the question of the best delivery route of corticoid as the anatomy of the nasal cavity is very different from human (Salazar et al., 2019). Previous studies have shown that corticoid treatments effectiveness to repair the OE after injury is very variable according to the pathophysiological context. Indeed studies in rodent models have shown that they can be detrimental to the OE regeneration (Crisafulli et al., 2018; Wang et al., 2021; Li et al., 2023) or beneficial (Sultan et al., 2011; Huang et al., 2019) and this may be related to the acknowledged role of macrophages in OE regeneration (Borders et al., 2007). Overall, our results indicate that persistent inflammation may disturb the recovery of the mature olfactory neuron population and that early corticoid treatment improves the recovery from SARS-CoV-2 induced olfactory impairment. However, side effects of such treatment are not without consequences (Huart et al., 2021) and require further human studies considering that most patients will spontaneously recover part of their olfactory capacities (Whitcroft et al., 2023).

Declaration

Ethics approval and consent to participate: Not applicable.
Consent for publication: Not applicable.

Availability of data and material: Data will be made available upon reasonable request, not applicable for material.

Funding: NM is supported by INRAe SA department; ANR (Grant CORAR); ANRS (Grant UCRAH). LMN is supported by the FRM (Fond pour la recherche médicale). CB is supported by the "DIM One Health".

Authors contribution: Conceptualization NM, SLP and LMN Investigation: LMN, CB, ASA, OAG, JJ, BK, SLP, NM Formal analysis: LMN, CB and NM Writing: NM with input from all authors.

CRediT authorship contribution statement

Laetitia Merle-Nguyen: Formal analysis, Investigation, Methodology, Writing – review & editing. **Ophélie Ando-Grard:** Data curation, Investigation. **Clara Bourgon:** Formal analysis, Investigation. **Audrey St Albin:** Investigation. **Juliette Jacquelin:** Formal analysis, Investigation. **Bernard Klonjkowski:** Project administration, Writing – review & editing. **Sophie Le Poder:** Data curation, Investigation, Project administration, Writing – review & editing. **Nicolas Meunier:** Conceptualization, Formal analysis, Funding acquisition, Investigation, Methodology, Project administration, Supervision, Writing – original draft.

Declaration of competing interest

The authors declare that they have no known competing financial interests or personal relationships that could have appeared to influence the work reported in this paper.

Data availability

Data will be made available on request.

Acknowledgment

We would like to thank all VIM members for their helpful discussion, Christopher von Bartheld for very helpful suggestions and global improvement of the manuscript, all the people from the PRBM platform of ENVA who helped us in the BSL3 animal facility.

Appendix A. Supplementary data

Supplementary data to this article can be found online at https://doi.org/10.1016/j.bbi.2024.02.020.

References

Bergman, U., Ostergren, A., Gustafson, A.L., Brittebo, B., 2002. Differential effects of olfactory toxicants on olfactory regeneration. Arch. Toxicol. 76, 104–112. https://doi.org/10.1007/s00204-002-0321-2.

Borders, A.S., Hersh, M.A., Getchell, M.L., van Rooijen, N., Cohen, D.A., Stromberg, A.J., Getchell, T.V., 2007. Macrophage-mediated neuroprotection and neurogenesis in the olfactory epithelium. Physiol. Genomics 31, 531–543. https://doi.org/10.1152/physiolgenomics.00008.2007.

Bourgon, C., Albin, A.S., Ando-Grard, O., Da Costa, B., Domain, R., Korkmaz, B., Klonjkowski, B., Le Poder, S., Meunier, N., 2022. Neutrophils play a major role in the destruction of the olfactory epithelium during SARS-CoV-2 infection in hamsters. Cell. Mol. Life Sci. 79, 616. https://doi.org/10.1007/s00018-022-04643-1.

Bozza, T., Feinstein, P., Zheng, C., Mombaerts, P., 2002. Odorant receptor expression defines functional units in the mouse olfactory system. J. Neurosci. 22, 3033–3043 https://doi.org/20026321 22/8/3033 [pii].

Bryche, B., Fretaud, M., Saint-Albin Deliot, A., Galloux, M., Sedano, L., Langevin, C., Descamps, D., Rameix-Welti, M.A., Eleouet, J.F., Le Goffic, R., Meunier, N., 2019. Respiratory syncytial virus tropism for olfactory sensory neurons in mice. J. Neurochem., e14936 https://doi.org/10.1111/jnc.14936.

Bryche, B., St Albin, A., Murri, S., Lacôte, S., Pulido, C., Ar Gouilh, M., Lesellier, S., Servat, A., Wasniewski, M., Picard-Meyer, E., Monchatre-Leroy, E., Volmer, R., Rampin, O., Le Goffic, R., Marianneau, P., Meunier, N., 2020. Massive transient damage of the olfactory epithelium associated with infection of sustentacular cells by SARS-CoV-2 in golden Syrian hamsters. Brain Behav. Immun. 89, 579–586. https://doi.org/10.1016/j.bbi.2020.06.032.

Butowt, R., Bilinska, K., von Bartheld, C.S., 2023. Olfactory dysfunction in COVID-19: new insights into the underlying mechanisms. Trends Neurosci. 46, 75–90. https://doi.org/10.1016/j.tins.2022.11.003.

Chen, M., Reed, R.R., Lane, A.P., 2019. Chronic inflammation directs an olfactory stem cell functional switch from neuroregeneration to immune defense. Cell Stem Cell 25 (501–513), e5.

Crisafulli, U., Xavier, A.M., Dos Santos, F.B., Cambiaghi, T.D., Chang, S.Y., Porcionatto, M., Castilho, B.A., Malnic, B., Glezer, I., 2018. Topical dexamethasone administration impairs protein synthesis and neuronal regeneration in the olfactory epithelium. Front. Mol. Neurosci. 11, 50. https://doi.org/10.3389/fnmol.2018.00050.

Dallman, M.F., la Fleur, S.E., Pecoraro, N.C., Gomez, F., Houshyar, H., Akana, S.F., 2004. Minireview: glucocorticoids—food intake, abdominal obesity, and wealthy nations in 2004. Endocrinology 145, 2633–2638. https://doi.org/10.1210/en.2004-0037.

Doty, R.L., Shaman, P., Kimmelman, C.P., Dann, M.S., 1984. University of pennsylvania smell identification test: A rapid quantitative olfactory function test for the clinic. Laryngoscope 94, 176–178. https://doi.org/10.1288/00005537-198402000-00004.

Etzerodt, A., Moestrup, S.K., 2013. CD163 and inflammation: biological, diagnostic, and therapeutic aspects. Antioxid. Redox Signal. 18, 2352–2363. https://doi.org/10.1089/ars.2012.4834.

Finlay, J.B., Brann, D.H., Abi Hachem, R., Jang, D.W., Oliva, A.D., Ko, T., Gupta, R., Wellford, S.A., Moseman, E.A., Jang, S.S., Yan, C.H., Matsunami, H., Tsukahara, T., Datta, S.R., Goldstein, B.J., 2022. Persistent post–COVID-19 smell loss is associated with immune cell infiltration and altered gene expression in olfactory epithelium. Sci. Transl. Med. 14, eadd0484 https://doi.org/10.1126/scitranslmed.add0484.

Frosolini, A., Parrino, D., Fabbris, C., Fantin, F., Inches, I., Invitto, S., Spinato, G., Filippis, C., 2022. Magnetic resonance imaging confirmed olfactory bulb reduction in long COVID-19: literature review and case series. Brain Sci. 12, 430. https://doi.org/10.3390/brainsci12040430.

Hintschich, C.A., Dietz, M., Haehner, A., Hummel, T., 2022. Topical administration of mometasone is not helpful in post-COVID-19 olfactory dysfunction. Life 12, 1483. https://doi.org/10.3390/life12101483.

Hosseinpoor, M., Kabiri, M., Rajati Haghi, M., Ghadam Soltani, T., Rezaei, A., Faghfouri, A., Poustchian Gholkhatmi, Z., Bakhshaee, M., 2022. Intranasal Corticosteroid Treatment on Recovery of Long-Term Olfactory Dysfunction Due to COVID -19. The Laryngoscope lary.30353. https://doi.org/10.1002/lary.30353.

Huang, J.S., Kunkhyen, T., Rangel, A.N., Brechbill, T.R., Gregory, J.D., Winson-Bushby, E.D., Liu, B., Avon, J.T., Muggleton, R.J., Cheetham, C.E.J., 2022. Immature olfactory sensory neurons provide behaviourally relevant sensory input to the olfactory bulb. Nat. Commun. 13, 6194. https://doi.org/10.1038/s41467-022-33967-6.

Huang, Z., Velasquez, N., Nguyen, A., Ye, T., Le, W., Bravo, D.T., Hwang, P.H., Zhou, B., Nayak, J.V., 2019. Topical corticosteroid pretreatment mitigates cellular damage after caustic injury to the nasal upper airway epithelium. Am. J. Rhinol. Allergy 33, 277–285. https://doi.org/10.1177/1945892418823305.

Huart, C., Philpott, C.M., Altundag, A., Fjaeldstad, A.W., Frasnelli, J., Gane, S., Hsieh, J. W., Holbrook, E.H., Konstantinidis, I., Landis, B.N., Macchi, A., Mueller, C.A., Negoias, S., Pinto, J.M., Poletti, S.C., Ramakrishnan, V.R., Rombaux, P., Vodicka, J., Welge-Lüessen, A., Whitcroft, K.L., Hummel, T., 2021. Systemic corticosteroids in coronavirus disease 2019 (COVID-19)-related smell dysfunction: an international view. Int. Forum Allergy Rhinol. 11, 1041–1046. https://doi.org/10.1002/alr.22788.

Jablonski, K.A., Amici, S.A., Webb, L.M., Ruiz-Rosado, J.D.D., Popovich, P.G., Partida-Sanchez, S., Guerau-de-Arellano, M., 2015. Novel markers to delineate murine M1 and M2 macrophages. PLoS One 10, e0145342.

Khan, M., Yoo, S.-J., Clijsters, M., Backaert, W., Vanstapel, A., Speleman, K., Lietaer, C., Choi, S., Hether, T.D., Marcelis, L., Nam, A., Pan, L., Reeves, J.W., Van Bulck, P., Zhou, H., Bourgeois, M., Debaveye, Y., De Munter, P., Gunst, J., Jorissen, M., Lagrou, K., Lorent, N., Neyrinck, A., Peetermans, M., Thal, D.R., Vandenbriele, C., Wauters, J., Mombaerts, P., Van Gerven, L., 2021. Visualizing in deceased COVID-19 patients how SARS-CoV-2 attacks the respiratory and olfactory mucosae but spares the olfactory bulb. S0092867421012824 Cell. https://doi.org/10.1016/j.cell.2021.10.027.

Kishimoto-Urata, M., Urata, S., Kagoya, R., Imamura, F., Nagayama, S., Reyna, R.A., Maruyama, J., Yamasoba, T., Kondo, K., Hasegawa-Ishii, S., Paessler, S., 2022. Prolonged and extended impacts of SARS-CoV-2 on the olfactory neurocircuit. Sci. Rep. 12, 5728. https://doi.org/10.1038/s41598-022-09731-7.

Le Bon, S.D., Konopnicki, D., Pisarski, N., Prunier, L., Lechien, J.R., Horoi, M., 2021. Efficacy and safety of oral corticosteroids and olfactory training in the management of COVID-19-related loss of smell. Eur. Arch. Otorhinolaryngol. https://doi.org/10.1007/s00405-020-06520-8.

Li, P., Wang, N., Kai, L., Si, J., Wang, Z., 2023. Chronic intranasal corticosteroid treatment induces degeneration of olfactory sensory neurons in normal and allergic rhinitis mice. Int Forum Allergy Rhinol 13, 1889–1905. https://doi.org/10.1002/alr.23142.

McGann, J.P., 2017. Poor human olfaction is a 19th-century myth. Science 356. https://doi.org/10.1126/science.aam7263.

Meunier, N., Briand, L., Jacquin-Piques, A., Brondel, L., Pénicaud, L., 2021. COVID 19-induced smell and taste impairments: putative impact on physiology. Front. Physiol. 11 https://doi.org/10.3389/fphys.2020.625110.

Moon, C., Yoo, J.Y., Matarazzo, V., Sung, Y.K., Kim, E.J., Ronnett, G.V., 2002. Leukemia inhibitory factor inhibits neuronal terminal differentiation through STAT3 activation. PNAS 99, 9015–9020.

Mori, E., Merkonidis, C., Cuevas, M., Gudziol, V., Matsuwaki, Y., Hummel, T., 2016. The administration of nasal drops in the "Kaiteki" position allows for delivery of the drug

to the olfactory cleft: a pilot study in healthy subjects. Eur. Arch. Otorhinolaryngol. 273, 939–943. https://doi.org/10.1007/s00405-015-3701-y.
Muller, P.Y., Janovjak, H., Miserez, A.R., Dobbie, Z., 2002. Processing of gene expression data generated by quantitative real-time RT-PCR. Biotechniques 32, 1372–1374, 1376, 1378–1379.
Nag, A.K., Saltagi, A.K., Saltagi, M.Z., Wu, A.W., Higgins, T.S., Knisely, A., Ting, J.Y., Illing, E.A., 2023. Management of post-infectious anosmia and hyposmia: a systematic review. Ann. Otol. Rhinol. Laryngol. 132, 806–817. https://doi.org/10.1177/00034894221118186.
Nakashima, N., Nakashima, K., Taura, A., Takaku-Nakashima, A., Ohmori, H., Takano, M., 2020. Olfactory marker protein directly buffers cAMP to avoid depolarization-induced silencing of olfactory receptor neurons. Nat. Commun. 11, 2188. https://doi.org/10.1038/s41467-020-15917-2.
Ohta, Y., Ichimura, K., 2000. Proliferation markers, proliferating cell nuclear antigen, Ki67, 5-bromo-2'-deoxyuridine, and cyclin D1 in mouse olfactory epithelium. Ann. Otol. Rhinol. Laryngol. 109, 1046–1048.
Okumura, S., Saito, T., Okazaki, K., Fushimi, K., Tsuzuki, K., 2022. Clinical features of olfactory dysfunction in elderly patients. S0385814622001638 Auris Nasus Larynx. https://doi.org/10.1016/j.anl.2022.06.001.
Orecchioni, M., Ghosheh, Y., Pramod, A.B., Ley, K., 2019. Macrophage polarization: different gene signatures in M1(LPS+) vs. classically and M2(LPS–) vs. alternatively activated macrophages. Front. Immunol. 10, 1084. https://doi.org/10.3389/fimmu.2019.01084.
Pendolino, A.L., Ottaviano, G., Nijim, J., Scarpa, B., De Lucia, G., Berro, C., Nicolai, P., Andrews, P.J., 2022. A multicenter real-life study to determine the efficacy of corticosteroids and olfactory training in improving persistent COVID -19-related olfactory dysfunction. Laryngoscope Investig Oto lio2.989. https://doi.org/10.1002/lio2.989.
Pieniak, M., Oleszkiewicz, A., Avaro, V., Calegari, F., Hummel, T., 2022. Olfactory training – Thirteen years of research reviewed. Neurosci. Biobehav. Rev. 141, 104853 https://doi.org/10.1016/j.neubiorev.2022.104853.
Porter, A.G., Janicke, R.U., 1999. Emerging roles of caspase-3 in apoptosis. Cell Death Differ. 6, 99–104.
Ramakrishnan, M.A., 2016. Determination of 50% endpoint titer using a simple formula. WJV 5, 85. https://doi.org/10.5501/wjv.v5.i2.85.
Rashid, R.A., Zgair, A., Al-Ani, R.M., 2021. Effect of nasal corticosteroid in the treatment of anosmia due to COVID-19: A randomised double-blind placebo-controlled study. Am. J. Otolaryngol. 42, 103033 https://doi.org/10.1016/j.amjoto.2021.103033.
Reyna, R.A., Kishimoto-Urata, M., Urata, S., Makishima, T., Paessler, S., Maruyama, J., 2022. Recovery of anosmia in hamsters infected with SARS-CoV-2 is correlated with repair of the olfactory epithelium. Sci. Rep. 12, 628. https://doi.org/10.1038/s41598-021-04622-9.
Rutkai, I., Mayer, M.G., Hellmers, L.M., Ning, B., Huang, Z., Monjure, C.J., Coyne, C., Silvestri, R., Golden, N., Hensley, K., Chandler, K., Lehmicke, G., Bix, G.J., Maness, N.J., Russell-Lodrigue, K., Hu, T.Y., Roy, C.J., Blair, R.V., Bohm, R., Doyle-Meyers, L.A., Rappaport, J., Fischer, T., 2022. Neuropathology and virus in brain of SARS-CoV-2 infected non-human primates. Nat. Commun. 13, 1745. https://doi.org/10.1038/s41467-022-29440-z.
Salazar, I., Sanchez-Quinteiro, P., Barrios, A.W., Lopez Amado, M., Vega, J.A., 2019. Anatomy of the olfactory mucosa. Handb. Clin. Neurol. 164, 47–65. https://doi.org/10.1016/B978-0-444-63855-7.00004-6.
Schwob, J.E., Jang, W., Holbrook, E.H., Lin, B., Herrick, D.B., Peterson, J.N., Hewitt Coleman, J., 2017. Stem and progenitor cells of the mammalian olfactory epithelium: Taking poietic license. J Comp Neurol 525, 1034–1054. https://doi.org/10.1002/cne.24105.
Sultan, B., May, L.A., Lane, A.P., 2011. The role of TNF-α in inflammatory olfactory loss. Laryngoscope 121, 2481–2486. https://doi.org/10.1002/lary.22190.
Suzuki, Y., Farbman, A.I., 2000. Tumor necrosis factor-α-induced apoptosis in olfactory epithelium in vitro: possible roles of caspase 1 (ICE), caspase 2 (ICH-1), and caspase 3 (CPP32). Exp. Neurol. 165, 35–45. https://doi.org/10.1006/exnr.2000.7465.
Takenouchi, T., Morozumi, T., Wada, E., Suzuki, S., Nishiyama, Y., Sukegawa, S., Uenishi, H., 2021. Dexamethasone enhances CD163 expression in porcine IPKM immortalized macrophages. In Vitro Cell. Dev. Biol. -Animal 57, 10–16. https://doi.org/10.1007/s11626-020-00535-5.
Tan, B.K.J., Han, R., Zhao, J.J., Tan, N.K.W., Quah, E.S.H., Tan, C.J.-W., Chan, Y.H., Teo, N.W.Y., Charn, T.C., See, A., Xu, S., Chapurin, N., Chandra, R.K., Chowdhury, N., Butowt, R., von Bartheld, C.S., Kumar, B.N., Hopkins, C., Toh, S.T., 2022. Prognosis and persistence of smell and taste dysfunction in patients with covid-19: meta-analysis with parametric cure modelling of recovery curves. BMJ e069503. https://doi.org/10.1136/bmj-2021-069503.
Thébault, S., Lejal, N., Dogliani, A., Donchet, A., Urvoas, A., Valerio-Lepiniec, M., Lavie, M., Baronti, C., Touret, F., Da Costa, B., Bourgon, C., Fraysse, A., Saint-Albin-Deliot, A., Morel, J., Klonjkowski, B., de Lamballerie, X., Dubuisson, J., Roussel, A., Minard, P., Le Poder, S., Meunier, N., Delmas, B., 2022. Biosynthetic proteins targeting the SARS-CoV-2 spike as anti-virals. PLoS Pathog. 18, e1010799.
Tragoonrungsea, J., Tangbumrungtham, N., Nitivanichsakul, T., Roongpuvapaht, B., Tanjararak, K., 2023. Corticosteroid nasal irrigation as early treatment of olfactory dysfunction in COVID-19: A prospective randomised controlled trial. Clin. Otolaryngol. 48, 182–190. https://doi.org/10.1111/coa.14004.
Vaira, L.A., Hopkins, C., Petrocelli, M., Lechien, J.R., Cutrupi, S., Salzano, G., Chiesa-Estomba, C.M., Saussez, S., De Riu, G., 2021. Efficacy of corticosteroid therapy in the treatment of long- lasting olfactory disorders in COVID-19 patients. Rhinology 59, 21–25. https://doi.org/10.4193/Rhin20.515.
Van Regemorter, V., Hummel, T., Rosenzweig, F., Mouraux, A., Rombaux, P., Huart, C., 2020. Mechanisms Linking Olfactory Impairment and Risk of Mortality. Front. Neurosci. 14, 140. https://doi.org/10.3389/fnins.2020.00140.
Verhaagen, J., Oestreicher, A.B., Gispen, W.H., Margolis, F.L., 1989. The expression of the growth associated protein B50/GAP43 in the olfactory system of neonatal and adult rats. J. Neurosci. 9, 683–691.
Verma, A.K., Zheng, J., Meyerholz, D.K., Perlman, S., 2022. SARS-CoV-2 infection of sustentacular cells disrupts olfactory signaling pathways. JCI Insight 7, e160277.
von Bartheld, C.S., Hagen, M.M., Butowt, R., 2021. The D614G virus mutation enhances anosmia in COVID-19 patients: evidence from a systematic review and meta-analysis of studies from South Asia. ACS Chem. Nerosci. 12, 3535–3549. https://doi.org/10.1021/acschemneuro.1c00542.
von Bartheld, C.S., Wang, L., 2023. Prevalence of olfactory dysfunction with the omicron variant of SARS-CoV-2: A systematic review and meta-analysis. Cells 12, 430. https://doi.org/10.3390/cells12030430.
Wang, L., Ren, W., Li, X., Zhang, X., Tian, H., Bhattarai, J.P., Challis, R.C., Lee, A.C., Zhao, S., Yu, H., Ma, M., Yu, Y., 2021. Chitinase-like protein Ym2 (Chil4) regulates regeneration of the olfactory epithelium via interaction with inflammation. J. Neurosci. 41, 5620–5637. https://doi.org/10.1523/JNEUROSCI.1601-20.2021.
Whitcroft, K.L., Altundag, A., Balungwe, P., Boscolo-Rizzo, P., Douglas, R., Enecilla, M.L. B., Fjaeldstad, A.W., Fornazieri, M.A., Frasnelli, J., Gane, S., Gudziol, H., Gupta, N., Haehner, A., Hernandez, A.K., Holbrook, E.H., Hopkins, C., Hsieh, J.W., Huart, C., Husain, S., Kamel, R., Kim, J.K., Kobayashi, M., Konstantinidis, I., Landis, B.N., Lechner, M., Macchi, A., Mazal, P.P., Miri, I., Miwa, T., Mori, E., Mullol, J., Mueller, C.A., Ottaviano, G., Patel, Z.M., Philpott, C., Pinto, J.M., Ramakrishnan, V. R., Roth, Y., Schlosser, R.J., Stjärne, P., Van Gerven, L., Vodicka, J., Welge-Luessen, A., Wormald, P.J., Hummel, T., 2023. Position paper on olfactory dysfunction: 2023. Rhinology. https://doi.org/10.4193/Rhin22.483.
Wyler, E., Adler, J.M., Eschke, K., Teixeira Alves, G., Peidli, S., Pott, F., Kazmierski, J., Michalick, L., Kershaw, O., Bushe, J., Andreotti, S., Pennitz, P., Abdelgawad, A., Postmus, D., Goffinet, C., Kreye, J., Reincke, S.M., Prüss, H., Blüthgen, N., Gruber, A. D., Kuebler, W.M., Witzenrath, M., Landthaler, M., Nouailles, G., Trimpert, J., 2022. Key benefits of dexamethasone and antibody treatment in COVID-19 hamster models revealed by single-cell transcriptomics. S1525001622001733 Mol. Ther.. https://doi.org/10.1016/j.ymthe.2022.03.014.
Yang, M., Crawley, J.N., 2009. Simple behavioral assessment of mouse olfaction. Current protocols in neuroscience Chapter 8, Unit 8 24. https://doi.org/10.1002/0471142301.ns0824s48.
Yang, Z., Ming, X.-F., 2014. Functions of arginase isoforms in macrophage inflammatory responses: impact on cardiovascular diseases and metabolic disorders. Front. Immunol. 5 https://doi.org/10.3389/fimmu.2014.00533.
Yuan, L., Zhou, M., Ma, J., Liu, X., Chen, P., Zhu, H., Tang, Q., Cheng, T., Guan, Y., Xia, N., 2022. Dexamethasone ameliorates severe pneumonia but slightly enhances viral replication in the lungs of SARS-CoV-2-infected Syrian hamsters. Cell. Mol. Immunol. 19, 290–292. https://doi.org/10.1038/s41423-021-00793-7.
Zazhytska, M., Kodra, A., Hoagland, D.A., Frere, J., Fullard, J.F., Shayya, H., McArthur, N.G., Moeller, R., Uhl, S., Omer, A.D., Gottesman, M.E., Firestein, S., Gong, Q., Canoll, P.D., Goldman, J.E., Roussos, P., tenOever, B.R., Overdevest, J.B., Lomvardas, S., 2022. Non-cell-autonomous disruption of nuclear architecture as a potential cause of COVID-19-induced anosmia. S0092867422001350 Cell. https://doi.org/10.1016/j.cell.2022.01.024.